

JPET #84103

**A-425619, a Novel and Selective TRPV1 Receptor Antagonist, Blocks  
Channel Activation by Vanilloids, Heat and Acid.**

Rachid El Kouhen, Carol S. Surowy, Bruce R. Bianchi, Torben R. Neelands,  
Heath A. McDonald, Wende Niforatos, Arthur Gomtsyan, Chih-Hung Lee, Prisca  
Honore, James P. Sullivan, Michael F. Jarvis and Connie R. Faltynek

Neuroscience Research  
Global Pharmaceutical Research and Development  
Abbott Laboratories  
Abbott Park, IL 60064-6123

JPET #84103

Running title: Characterization of A-425619 as a novel TRPV1 antagonist.

Correspondence and reprints to:

Rachid El Kouhen, Ph.D.

Abbott Laboratories

R4PM. AP9A/2. 100 Abbott Park Rd.

Abbott Park, IL 60064-6123

Tel. 847 935 5305

Fax. 847 937 9195

rachid.elkouhen@abbott.com

Text pages: 32

Tables: 3

Figures: 9

References: 32

Abstract: 196

Introduction: 415

Discussion: 794

Abbreviations: TRPV1, transient receptor potential vanilloid 1; FLIPR, fluorometric imaging plate reader; I-RTX, 5-iodo-resiniferatoxin; PDBu, phorbol-12, 13-dibutyrate; NADA, *N*-arachidonoyl-dopamine.

Recommended section: Neuropharmacology

## **Abstract**

The vanilloid receptor TRPV1 integrates responses to multiple stimuli, such as capsaicin, acid, heat and endovanilloids, and plays an important role in the transmission of inflammatory pain. Here, we report the identification and *in vitro* characterization of A-425619 (1-isoquinolin-5-yl-3-(4-trifluoromethyl-benzyl)-urea), a novel, potent and selective, TRPV1 antagonist. A-425619 was found to potently block capsaicin-evoked increases in intracellular calcium concentrations in HEK293 cells expressing recombinant human TRPV1 receptors ( $IC_{50} = 5$  nM). A-425619 showed similar potency ( $IC_{50} = 3-4$  nM) to block TRPV1 receptor activation by anandamide and N-arachidonoyl-dopamine. Electrophysiological experiments showed that A-425619 also potently blocked the activation of native TRPV1 channels in rat dorsal root ganglion neurons ( $IC_{50} = 9$  nM). When compared to other known TRPV1 antagonists, A-425619 exhibited superior potency in blocking both naive and phorbol ester-sensitized TRPV1 receptors. Like capsazepine, A-425619 demonstrated competitive antagonism ( $pA_2 = 2.5$  nM) of capsaicin evoked calcium flux. Moreover, A-425619 was 25-50-fold more potent than capsazepine in blocking TRPV1 activation. A-425619 showed no significant interaction with a wide range of receptors, enzymes and ion channels, indicating a high degree of selectivity for TRPV1 receptors. These data show that A-425619 is a structurally novel, potent and selective TRPV1 antagonist.

The vanilloid receptor VR1, recently termed TRPV1, is a non-selective cation channel predominantly expressed by peripheral nociceptors. TRPV1 receptors are readily activated by noxious chemicals, such as capsaicin and resiniferatoxin, protons ( $\text{pH} < 6.0$ ), and noxious heat ( $> 43^{\circ}\text{C}$ ) (Caterina et al., 1997; Tominaga et al., 1998). TRPV1 is also activated or potentiated by endovanilloids, such as anandamide, *N*-arachidonoyl-dopamine (NADA) (Huang et al., 2002), and *N*-oleoyl-dopamine (OLDA) (Chu et al., 2003) as well as eicosanoids, such as 12-HPETE (Hwang et al., 2000).

An interesting property of this channel is that these diverse stimuli not only directly activate TRPV1, but also sensitize and reduce the activation thresholds of the channel to other stimuli (Di Marzo et al., 2002). For example, exposure of TRPV1-expressing cells to acidic conditions sensitizes the channel to activation by heat or by capsaicin (Tominaga et al., 1998). In addition, several studies have shown that TRPV1 receptors can be sensitized by inflammatory agents, including bradykinin, NGF and ATP, acting *via* second messengers downstream of receptors for these agents (Cortright and Szallasi, 2004). Direct activation of PKC by phorbol 12-myristate 13-acetate (PMA) or phorbol-12, 13-dibutyrate (PDBu) leads to similar sensitization of TRPV1 responses to other stimuli (Di Marzo et al., 2002; El Kouhen et al., 2003). These data suggest that TRPV1 plays a key role in the integration of noxious signals after inflammation or tissue injury.

The prototypic TRPV1 receptor antagonist, capsazepine, has been extensively studied and shown to inhibit nocifensive and hyperalgesic responses

JPET #84103

not only to capsaicin, but also to inflammatory agents (Nagy et al., 2004). However, capsazepine has only modest potency and low specificity, also antagonizing voltage-activated calcium channels (Docherty et al., 1997), acetylcholine receptors (Liu & Simon, 1997), and hyperpolarizing-activated cyclic nucleotide-gated channels such as HCN1 (Gill et al., 2004). Efforts from several groups have been directed to the development of novel TRPV1 receptor antagonists with improved potency and/or selectivity compared to capsazepine. For example, arginine-rich peptides have been reported as TRPV1 blockers with analgesic activities (Planells-Cases et al., 2000). Other TRPV1 antagonists have been described recently, including *N*-(4-Tertiarybutylphenyl)-4-(3-cholorphyrin-2-yl)tetrahydropyrazine-1(2*H*)-carbox-amide (BCTC)(Valenzano et al., 2003), JYL1421 and KJM429 (Wang et al., 2002), SB-366791 (Gunthorpe et al., 2004), *N*-(4-chlorobenzyl) -*N'*-(4-hydroxy-3-iodo-5-methoxybenzyl)thiourea (IBTU)(Toth et al., 2004), 4-(3-Trifluoromethylpyridin-2-yl)piperazine-1-carboxylic Acid (5-Trifluoromethyl pyridin -2-yl)amide (Compound 41)(Swanson et al. 2005), (E)-3-(4-*t*-butylphenyl)-*N*-(2,3-dihydrobenzo[*b*][1,4]dioxin-6-yl)acrylamide (AMG9810)(Doherty et al., 2005), and 5-iodo-resiniferatoxin (Wahl et al., 2001).

The present studies were carried out to characterize a novel TRPV1 receptor antagonist A-425619 (1-isoquinolin-5-yl-3-(4-trifluoromethyl-benzyl)-urea) that was optimized from hits identified by high throughput screening of chemical libraries (Gomtsyan et al., 2005).

## **Methods**

**Materials.** Cell culture media and fetal bovine serum were obtained from Sigma-Aldrich Corp. (St. Louis, MO). G418 sulfate was obtained from Calbiochem-Novabiochem Corp. (San Diego, CA). Dulbecco's phosphate-buffered saline, pH 7.4 (D-PBS)(with calcium, magnesium, and 1 mg/ml D-glucose) was obtained from Gibco BRL (Grand Island, NY). Fluo-4 AM was purchased from Tef Labs (Austin, TX). NADA was purchased from Tocris (Ellisville, MO). A-425619 was synthesized at Abbott Laboratories (Abbott Park, IL). All other chemicals were obtained from Sigma-Aldrich (St. Louis, MO), unless otherwise indicated.

**Ca<sup>2+</sup> flux assay.** Cloning and stable expression of the human TRPV1 receptor in HEK293 cells have been previously detailed (Witte et al., 2002). TRPV1 mediated elevation of intracellular calcium levels was measured using the fluorescent calcium chelating dye fluo-4, as described previously (Smart et al., 2001). Briefly, cells were grown as a monolayer in black-walled clear bottom 96-well Biocoat<sup>TM</sup> plates (precoated with poly-D-lysine)(BD Biosciences, Bedford, MA). Growth medium was comprised of Dulbecco's modified Eagle medium (D-MEM)(with 4.5 mg/ml D-glucose), 4 mM L-glutamine, 300 µg/ml G-418 sulfate and 10% (v/v) fetal bovine serum. Prior to start of the assay, the cells were incubated with 2 µM (acetyloxy)methyl ester form of fluo-4 (fluo-4 AM) in D-PBS for 2 hr at 25°C. Subsequently, cells were washed with D-PBS to remove extracellular fluo-4 AM, and 100-150 µl D-PBS were added to each well. In some experiments, cells were pretreated with 100 nM phorbol 12,13-dibutyrate (PDBu)

JPET #84103

in D-PBS for 20 min at 25°C to sensitize TRPV1 to capsaicin, NADA or heat. All test compounds were dissolved in DMSO (10 mM stocks), except NADA (5 mg/ml in ethanol) and ruthenium red (10 mM in dH<sub>2</sub>O), and then diluted in D-PBS to obtain (4X) solutions. Test compounds (50 µl of the (4X) solutions) were added to the cells at a delivery rate of 50 µl/s. Antagonists were added to the cells 5 min before addition of agonist, and final assay volume was 200 µl. Acid activation studies of the TRPV1 receptor were performed in a similar manner, except ambient pH was lowered to pH 6.7 to facilitate detection of a pure TRPV1-mediated increased intracellular Ca<sup>2+</sup>. Antagonist solutions were prepared in the ambient pH buffer. Acidic pH solutions were prepared by titration of D-PBS with 1 M HCl, and then 50 µl were added to the cells at a delivery rate of 50 µl/s. For heat activation studies, the liquid contents of the wells were aspirated and replaced with 50 µl of D-PBS or test compound solution at ambient room temperature (25°C). A 96-well assay plate of D-PBS (250 µl per well) was preheated on a hot orbital shaker (Daigger, Vernon Hills, IL) to 50°C, and then 150 µl of heated solution were added to the cells at a delivery rate of 50 µl/s to attain a peak temperature of 38°C. Peak temperature was determined using a TH-1 Therm probe (Cell MicroControls, Norfolk, VA). Changes in fluorescence were recorded over time in a fluorometric imaging plate reader (FLIPR)(Molecular Devices Corp., Sunnyvale, CA)( $\lambda_{EX} = 488 \text{ nm}$ ,  $\lambda_{EM} = 540 \text{ nm}$ ). Antagonists were tested at 11 concentrations (indicated on each graph). The peak increase in fluorescence over baseline (relative fluorescence units or RFU) was calculated, and expressed as a percentage of the maximal agonist response

JPET #84103

(in absence of antagonist).  $EC_{50}$  and  $IC_{50}$  values were calculated from curve-fits of the concentration-effect data using a four-parameter logistic Hill equation (GraphPad Prism<sup>®</sup>, GraphPad Software, Inc., San Diego, CA). Significant differences were calculated by unpaired, two-tailed Student T tests.

**DRG Neuronal Cultures.** Adult male Sprague-Dawley rats (~8 wk old, 250-300 g) were deeply anesthetized with CO<sub>2</sub> and sacrificed. Lumbar (L<sub>4</sub> – L<sub>6</sub>) DRG were dissected from the vertebral column and placed in Dulbecco's modified Eagles medium (DMEM)(Hyclone, Logan, UT) containing 0.3% collagenase B (Roche Molecular, Indianapolis, IN) for 60 min at 37°C. The collagenase was replaced with 0.25% trypsin (GIBCO-BRL, Grand Island, NY) in Ca<sup>2+</sup>/Mg<sup>2+</sup>-free Dulbecco's phosphate-buffered saline (PBS), and further digested for 30 min at 37°C. After washing in fresh DMEM, ganglia were dissociated by trituration using a fire-polished Pasteur pipette. Cells were washed in fresh DMEM and tritured again using a smaller bore fire-polished pipette to obtain a single-cell suspension. DRG cells were then plated on polyethelenimine (PEI)-treated 12 mm glass coverslips. Cells were plated at a density of one DRG per coverslip in 1 ml DMEM supplemented with 10% FBS, NGF (50 ng/ml), and 100 U/ml Pen/Strep. Neurons were used for electrophysiological recording within 12 – 24 h. Experimental procedures involving rats were conducted under a protocol approved by an Institutional Animal Care and Use Committee.

**Electrophysiology.** Rat DRGs were maintained at room temperature in an extracellular recording solution (pH 7.4, 325 mOsm) consisting of (in mM): 155 NaCl, 5 KCl, 2 CaCl<sub>2</sub>, 1 MgCl<sub>2</sub>, 10 HEPES, 12 glucose. Patch-pipettes

JPET #84103

composed of borosilicate glass (1B150F-3; World Precision Instruments, Inc, Sarasota, FL), were pulled and fire-polished using a DMZ-Universal micropipette puller (Zeitz-Instruments, Martinsried, Germany). Pipettes (2-6 M $\Omega$ ) were filled with an internal solution (pH 7.3, 295 mOsm) consisting of (in mM): 122.5 K-aspartate, 20 KCl, 1 MgCl<sub>2</sub>, 10 EGTA, 5 HEPES, 2 ATP•Mg. Standard whole-cell recording techniques were utilized for voltage-clamp studies using an Axopatch 200B amplifier (Axon Instruments, Foster City, CA)(Hamill et al., 1981).

Cells were continuously perfused with extracellular solution at a rate of 0.5 ml/min. Capsaicin was applied to small- to medium-sized neurons (25 – 35  $\mu$ m diameter) for 5 seconds using a piezoelectric-driven theta-tube application device (Burleigh Instruments, Fishers, NY) controlled by Axon Instruments pClamp 9 software (Axon Instruments, Foster City, CA). Control responses typically ran down for the first 5-10 minutes following whole-cell configuration. Therefore, capsaicin was applied alone at two minute intervals until successive applications produced currents of similar amplitude. At this point, increasing concentrations of A-425619 were pre-applied to the neuron for ~60 seconds, followed by co-application of capsaicin and A-425619. Peak current amplitudes were measured and plotted as a function of antagonist concentration. In a subset of neurons, the washout of the inhibition by A-425619 was monitored by continuing application of capsaicin at two minute intervals while applying external solution to the cell. Current amplitudes typically recovered to >80% of control responses within 4-6 minutes.

JPET #84103

For electrophysiological studies a 10 mM stock solution of A-425619 dissolved in DMSO was serially diluted 1:10 in DMSO. On the day of recording, the resulting stock solutions were diluted 1:1000 or 1:333 into external solution for the final concentrations. DMSO alone at these concentrations had no effect on capsaicin-activated currents.

## **Results**

### **Activation of human TRPV1 receptors stably expressed in HEK293 cells.**

Characterization of recombinant human TRPV1 receptors stably expressed in HEK293 cells was carried out using a  $\text{Ca}^{2+}$  flux-based assay (FLIPR) as previously reported (Witte et al., 2002; Smart et al., 2001). Fig. 1 shows representative FLIPR tracings following activation of TRPV1 receptors by different stimuli. Addition of 50 nM capsaicin, a concentration equivalent to  $\text{EC}_{50}$  (Fig. 2A), elicited a rapid and a robust increase in intracellular calcium concentrations with a maximum response obtained within 10-20 sec (Fig. 1A). Untransfected HEK293 cells (Null) showed no response to capsaicin. Concentrations equivalent to  $\text{EC}_{50}$ s of NADA (3  $\mu\text{M}$ ) and anandamide (10  $\mu\text{M}$ )(Fig. 2A) evoked a response similar to that evoked by capsaicin (Fig. 1B, C). Both anandamide and NADA behaved as less potent agonists at the TRPV1 receptor with maximum calcium signals occurring at 60-120 sec. Note that NADA and anandamide also produced small calcium signals (~ 10%) in Null HEK293 cells, indicating that these endogenous ligands evoked non-TRPV1 receptor mediated responses in addition to activating TRPV1 (Fig. 1B, C). Acid activation of TRPV1 receptors was performed by reducing the extracellular pH, as described in Methods. As shown in Fig. 1D, the acid (pH 5.5)-evoked increased intracellular calcium response was immediate and transient. This effect was specific to the TRPV1 receptor since no acid response was observed with Null HEK293 cells (Fig. 1D and Fig. 2B).

### ***In vitro* pharmacological characterization of A-425619.**

JPET #84103

*A-425619 is a highly potent antagonist at the recombinant human TRPV1 receptor.*

The abilities of A-425619 (1-isoquinolin-5-yl-3-(4-trifluoromethyl-benzyl)-urea) and other TRPV1 antagonists (Fig. 3) to inhibit receptor activation were investigated using HEK293 cells stably expressing human TRPV1 receptors. As shown in Fig. 4A, A-425619 blocked TRPV1 activation by 50 nM capsaicin in a concentration-dependent manner. A-425619 was a more potent antagonist ( $IC_{50}$  = 5 nM) than capsazepine ( $IC_{50}$  = 149 nM) or ruthenium red ( $IC_{50}$  = 512 nM)(Fig. 4A). Under the same conditions, A-425619 was 15-fold more potent than I-RTX ( $IC_{50}$  = 75 nM), in blocking TRPV1 receptor activation by capsaicin (Fig. 4A and Table 1).

A-425619 was also very potent in blocking TRPV1 activation by 3  $\mu$ M NADA ( $IC_{50}$  = 4 nM) or 10  $\mu$ M anandamide ( $IC_{50}$  = 3 nM), with a rank order of potencies of A-425619 > I-RTX > capsazepine > ruthenium red (Fig. 4B, C). However, the activation of TRPV1 receptor-mediated  $Ca^{2+}$  flux evoked by either NADA or anandamide was not completely inhibited by any of the TRPV1 receptor antagonists (Fig. 4B, C). These data are consistent with results obtained in null HEK293 cells (Fig. 1) which indicate that these ligands induced a small non-TRPV1 receptor mediated increased intracellular calcium in addition to activating TRPV1 receptors. This non-specific effect was more evident in the case of anandamide, where ~ 30% of the total response was unaffected by TRPV1 receptor antagonists (Fig. 4C).

A-425619 was highly potent in blocking activation of TRPV1 receptors by acid (pH 5.5)(Fig. 4D). The rank order of potencies was A-425619 (2 nM) > capsazepine (50 nM) > I-RTX (88 nM) > ruthenium red (386 nM)(Fig. 4D). The pIC<sub>50</sub> and Hill slope values for A-425619 and other antagonists in blocking TRPV1 activation by different stimuli are summarized in Table 1.

*A-425619 is a potent antagonist at the native rat TRPV1 receptor.*

The ability of A-425619 to block native TRPV1 receptor activation was examined electrophysiologically in cultured rat dorsal root ganglion (DRG) neurons, as described in Methods. Application of 1  $\mu$ M capsaicin to small diameter neurons clamped at  $-70$  mV elicited large inward currents. Capsaicin-evoked currents were reduced in the presence of A-425619 in a concentration-dependent manner (IC<sub>50</sub> = 9 nM) and were completely blocked at 100 nM (Fig. 5). TRPV1 receptor block by A-425619 was reversible since capsaicin-evoked currents were recovered following antagonist washout (Fig. 5A). Additionally, A-425619 was able to potently block the activation of TRPV1 receptors by endogenous ligands. 10  $\mu$ M anandamide elicited a large current that was fully blocked by 100 nM A-425619 (data not shown).

*A-425619 is a highly selective TRPV1 antagonist.*

In order to determine the specificity of A-425619, the compound was profiled in a large panel of *in vitro* binding assays (CEREP, Poitiers, France). These assays included G protein-coupled receptors (GPCRs), enzymes, transporters, and ion channels, and are listed in Table 2. A-425619 was found to be inactive (IC<sub>50</sub> > 10  $\mu$ M) at most of the tested targets. Additionally, A-425619 was weak or

JPET #84103

inactive in functional FLIPR-based assays against other targets, including P2X<sub>3</sub> (IC<sub>50</sub> > 10  $\mu$ M), P2X<sub>2/3</sub> (IC<sub>50</sub> > 10  $\mu$ M), TRPM8 (IC<sub>50</sub> = 8  $\mu$ M) and TRPA1 (IC<sub>50</sub> > 10  $\mu$ M) receptors. Thus, the present data demonstrate that A-425619 is a highly selective antagonist of TRPV1 receptors.

*A-425619 is a competitive antagonist at the TRPV1 receptor.*

To determine the nature of A-425619 antagonism at the TRPV1 receptor, capsaicin concentration-effect curves were determined in the presence of increasing concentrations of A-425619. Fig. 6A shows that capsaicin concentration-effect curves were shifted to the right with increasing A-425619 concentrations, without affecting the maximal capsaicin response. This indicates that A-425619 acts as a competitive antagonist at the TRPV1 receptor capsaicin-binding site. A Schild plot analysis yielded a pA<sub>2</sub> of 2.5 nM and a slope factor of  $1.06 \pm 0.05$  (Fig. 6B). Under the same conditions, concentration response curves for capsaicin were generated with increasing concentrations of capsazepine and ruthenium red. Consistent with competitive antagonism by capsazepine, capsaicin dose response curves were shifted to the right as a function of increasing concentrations of capsazepine, without change in the maximal responses (slope =  $1.16 \pm 0.08$ ) (Fig. 6C). In contrast, increasing concentrations of the antagonist ruthenium red induced a large decrease in the efficacy of capsaicin to stimulate calcium flux with a small rightward shift of the capsaicin dose response curves (Fig. 6D), consistent with non-competitive antagonism.

*A-425619 is a potent antagonist at the sensitized TRPV1 receptor.*

JPET #84103

Agents such as heat, acid and endovanilloids not only activate TRPV1 receptors but also sensitize the channel responses to other stimuli (Cortright and Szallasi, 2004). We recently reported that sensitization of TRPV1 under acidic conditions involves receptor phosphorylation and that PKC plays an important role in this acid-induced sensitization (El Kouhen et al., 2003). The ability of A-425619 to block the activation of sensitized TRPV1 receptors was investigated under different conditions. In the presence of 100 nM PDBu or pH 6.0, the potency of capsaicin to stimulate increased intracellular calcium was enhanced 2-4 fold (control capsaicin concentration-effect curves in the absence of antagonist, Fig. 7A, B).  $EC_{50}$  values for capsaicin were 8.5 nM and 15 nM, after PDBu and acid pretreatment, respectively (Fig. 7A, B). The  $EC_{50}$  value for capsaicin to activate the naive TRPV1 receptor was ~ 50 nM). In the presence of increasing concentrations of A-425619, concentration-effect curves of capsaicin were shifted to the right (Fig. 7A, B). Schild plot analysis yielded  $pA_2$  values of 0.8 nM and 4.3 nM after sensitization by PDBu and acid, respectively (Fig. 7C). These  $pA_2$  values were not significantly different ( $p > 0.05$ ) from that generated in naive conditions (2.5 nM)(Fig. 6B), and showed that A-425619 remained a potent antagonist at sensitized TRPV1 receptors. The rank order of potencies for antagonist block of sensitized TRPV1 was the same as that in blocking activation of naive TRPV1, A-425619 > I-RTX > capsazepine > ruthenium red (Fig. 8, Table 3).

The ability of heat to activate TRPV1 receptors was also assessed in the calcium flux assay on both naive and PDBu-sensitized channels, as described in

JPET #84103

**Methods.** A small but significant response was observed in TRPV1 receptor-expressing HEK293 cells in response to heat (38°C). This signal was dramatically increased when the cells were pretreated for 20 min with the PKC activator PDBu (100 nM)(Fig. 9A). However, the increased intracellular calcium evoked by heat in PDBu-treated cells (see Methods) was transient and much shorter in duration than that induced by other stimuli (Fig. 1). The transient nature of this response may be due, at least in part, to the methodology used as well as to the response of the channel to heat. The small heat-evoked signal obtained in Null cells was unaffected by the PDBu pretreatment (Fig. 9A). The ability of A-425619 and other antagonists to block the response of the sensitized TRPV1 receptor to heat was also examined. A-425619 effectively attenuated this response and was approximately 25-fold and 50-fold more potent than I-RTX and capsazepine, respectively (Fig. 9B and Table 3).

## ***Discussion***

The present data demonstrate that the structurally novel compound A-425619 is a highly potent TRPV1 receptor antagonist. A-425619 is a competitive antagonist of capsaicin-evoked receptor activation and can potently block both “naive” and sensitized TRPV1 receptor responses to a variety of stimuli. A-425619 is a potent antagonist at both recombinant human and native rat TRPV1 receptors and shows a high degree of specificity as compared to its activity at other cell surface receptors and ion channels.

It is now generally accepted that TRPV1 is an integrator of multiple and diverse stimuli, such as vanilloids, acid ( $\text{pH} < 6.0$ ), heat ( $> 43^{\circ}\text{C}$ ) and endogenous arachidonic acid derivatives (Caterina et al., 1997; Tominaga et al., 1998). These agents can directly activate TRPV1 receptors as well as sensitize channel responses to other noxious stimuli (Di Marzo et al., 2002). Moreover, inflammatory agents, including ATP, NGF and bradykinin can potentiate TRPV1 responses by activating specific kinases, which phosphorylate the TRPV1 channel (Di Marzo et al., 2002). Interestingly, both NGF and bradykinin also induce the hydrolysis of phosphatidylinositol (4,5)-biphosphate (PIP<sub>2</sub>), which leads to the release of TRPV1 receptor from an inhibited state (Chuang et al., 2001). These studies indicate that the TRPV1 channel is regulated by multiple mechanisms and support the importance of this channel in pain transmission during inflammation or tissue injury.

The present work demonstrates that the structurally novel TRPV1 receptor antagonist A-425619 is 25-50-fold more potent than capsazepine in blocking

JPET #84103

activation of TRPV1 receptors by a variety of stimuli, including capsaicin, acid, heat, NADA and anandamide. A-425619 completely blocked TRPV1 activation by capsaicin, acid and heat. However, the calcium flux induced by NADA and anandamide was not fully blocked by A-425619, consistent with previous reports, that NADA and anandamide have additional activities, including effects on fatty-acid amide hydrolase and cannabinoid CB1 receptors (Huang et al., 2002; Chu et al., 2003). Moreover, *in vitro* and *in vivo* studies with capsazepine have been difficult to interpret due to the low selectivity of this antagonist for blocking TRPV1 receptors (Nagy et al., 2004). Thus, the availability of highly potent and selective antagonists of TRPV1 receptors not only will help to elucidate the complex pharmacology of this interesting channel, but also may have therapeutic potential as novel analgesics.

Consistent with other reports, both acid and PDBu pretreatments reduced activation thresholds of TRPV1 receptors by capsaicin, heat, anandamide or NADA (Cortright and Szallasi, 2004; El Kouhen et al., 2003). Interestingly, here we provide evidence that A-425619 effectively blocked the activation of both naive and sensitized TRPV1 channels. Sensitization or phosphorylation of TRPV1 seems to increase the affinity of the channel to agonist e.g. capsaicin (Vellani et al., 2001; Premkumar and Ahern, 2000). However, a Schild plot analysis indicated that the affinity of A-425619 to block sensitized TRPV1 receptors remained comparable to that blocking naive TRPV1 receptors. The present data suggest that TRPV1 antagonists such as A-425619 may serve as

JPET #84103

an effective tool in blocking TRPV1 activation during inflammation or tissue injury.

Like capsazepine, A-425619 competitively blocked the ability of capsaicin to stimulate calcium flux through TRPV1 receptors. The capsaicin recognition site has been proposed to be predominantly localized on intracellular domains of TRPV1 (Jung et al., 1999; Jordt and Julius, 2002), although there is evidence of an extracellular domain as well (Vyklicky et al., 2003). In contrast, the proton interaction site is proposed to be extracellular (Jordt et al., 2000). Since A-425619 blocks activation of TRPV1 receptors by multiple stimuli, it is possible that this compound blocks or modulates the gating mechanism of the channel. It has been reported that the non-competitive antagonist ruthenium red blocks the activation of TRPV1 channels by different stimuli through blocking of the channel gating (Czirjak and Enyedi, 2003). Alternatively, protons and heat could act as TRPV1 modulators, by sensitizing the channel to activation by endogenous vanilloids. In this case, A-425619 would inhibit proton, heat or PDBu activation of TRPV1 by competing for recognition site(s) for capsaicin or endogenous vanilloids. Evidence supporting this latter interpretation comes from demonstrations that the potency and efficacy of anandamide to activate TRPV1 receptors is greatly enhanced under acidic conditions (Premkumar and Ahern, 2000; Vellani et al., 2001). Although, the exact mode by which capsaicin-competitive antagonists block TRPV1 receptor activation in response to other stimuli remains unclear, the present data demonstrate that A-425619 can effectively block TRPV1 receptor activation by a variety of pronociceptive stimuli

JPET #84103

and that the potency of this antagonist for TRPV1 receptors is largely unaffected by the state of channel activation. The present data show that A-425619 serves as a useful tool to enhance the understanding of the complex TRPV1 pharmacology. In addition, the structurally novel TRPV1 antagonist A-425619 will be useful in defining the analgesic potential of blockade of TRPV1 *in vivo* (Honore et al., companion manuscript).

JPET #84103

**References:**

Caterina MJ, Schumacher MA, Tominaga M, Rosen TA, Levine JD and Julius D (1997) The capsaicin receptor: a heat-activated ion channel in the pain pathway. *Nature* 389:816-824.

Chu CJ, Huang SM, De Petrocellis L, Bisogno T, Ewing SA, Miller JD, Zipkin RE, Daddario N, Appendino G, Di Marzo V and Walker JM (2003) N-oleoyldopamine, a novel endogenous capsaicin-like lipid that produces hyperalgesia. *J Biol Chem* 278:13633-13639.

Chuang HH, Prescott ED, Kong H, Shields S, Jordt SE, Basbaum AI, Chao MV and Julius D (2001) Bradykinin and nerve growth factor release the capsaicin receptor from PtdIns(4,5)P<sub>2</sub>-mediated inhibition. *Nature* 411:957-962.

Cortright DN and Szallasi A (2004) Biochemical pharmacology of the vanilloid receptor TRPV1. An update. *Eur J Biochem* 271:1814-1819.

Czirjak G and Enyedi P (2003) Ruthenium red inhibits TASK-3 potassium channel by interconnecting glutamate 70 of the two subunits. *Mol Pharmacol* 63:646-652.

Di Marzo V, Blumberg PM and Szallasi A (2002) Endovanilloid signaling in pain. *Curr Opin Neurobiol* 12:372-379.

Docherty RJ, Yeats JC and Piper AS (1997) Capsazepine block of voltage-activated calcium channels in adult rat dorsal root ganglion neurons in culture. *Br J Pharmacol* 121:1461-1467.

Doherty EM, Fotsch C, Bo Y, Chakrabarti PP, Chen N, Gavva N, Han N, Kelly MG, Kincaid J, Klionsky L, Liu Q, Ognyanov VI, Tamir R, Wang X, Zhu J, Norman MH and Treanor JJS (2005) Discovery of potent, orally available

JPET #84103

vanilloid receptor-1 antagonists. Structure-activity relationship of *N*-Aryl Cinnamides. *J Med Chem* 48:71-90.

El Kouhen R, Bianchi BR, Estvander BR, Surowy CS, Jarvis MF and Faltynek CR (2003) Correlation between phosphorylation and sensitization of the VR1 receptor. Program No. 811.4. *2003 Abstract Viewer and Itinerary Planner*. New Orleans, LA: Society for Neuroscience, Online.

Gill CH, Randall A, Bates SA, Hill K, Owen D, Larkman PM, Cairns W, Yusaf SP, Murdock PR, Strijbos PJ, Powell AJ, Benham CD and Davies CH (2004) Characterization of the human HCN1 channel and its inhibition by capsazepine. *Br J Pharmacol* 143:411-421.

Gomtsyan A, Bayburt EK, Schmidt RG, Zheng GZ, Perner RJ, Didomineco S, Koenig JR, Turner S, Jinkerson T, Drizin I, Hannick SM, Macri BS, McDonald HA, Honore P, Wismer CT, Marsh KC, Wetter J, Stewart KD, Oie T, Jarvis MF, Surowy CS, Faltynek CR and Lee CH (2005) Novel transient receptor potential vanilloid 1 (TRPV1) receptor antagonists for the treatment of pain: structure–activity relationships for ureas with quinoline, isoquinoline, quinazoline, phthalazine, quinoxaline and cinnoline moieties. *J Med Chem* 48:744-752.

Gunthorpe MJ, Rami HK, Jerman JC, Smart D, Gill CH, Soffin EM, Luis Hannan S, Lappin SC, Egerton J, Smith GD, Worby A, Howett L, Owen D, Nasir S, Davies CH, Thompson M, Wyman PA, Randall AD and Davis JB (2004) Identification and characterization of SB-366791, a potent and selective vanilloid receptor (VR1/TRPV1) antagonist. *Neuropharmacology* 46:133-149. Erratum in *Neuropharmacology* (2004) 46:905.

Hamill OP, Marty A, Neher E, Sakmann B and Sigworth FJ (1981) Improved patch-clamp techniques for high-resolution current recording from cells and cell-free membrane patches. *Pflugers Arch* 391:85-100.

JPET #84103

Huang SM, Bisogno T, Trevisani M, Al-Hayani A, De Petrocellis L, Fezza F, Tognetto M, Petros TJ, Krey JF, Chu CJ, Miller JD, Davies SN, Geppetti P, Walker JM and Di Marzo V (2002) An endogenous capsaicin-like substance with high potency at recombinant and native vanilloid VR1 receptors. *Proc Natl Acad Sci USA* 99:8400-8405.

Hwang SW, Cho H, Kwak J, Lee SY, Kang CJ, Jung J, Cho S, Min KH, Suh YG, Kim D and Oh U (2000) Direct activation of capsaicin receptors by products of lipoxygenases: endogenous capsaicin-like substances. *Proc Natl Acad Sci USA* 97:6155-6160.

Jordt SE and Julius D (2002) Molecular basis for species-specific sensitivity to "hot" chili peppers. *Cell* 108:421-430.

Jordt SE, Tominaga M and Julius D (2000) Acid potentiation of the capsaicin receptor determined by a key extracellular site. *Proc Natl Acad Sci USA* 97:8134-8139.

Jung J, Hwang SW, Kwak J, Lee SY, Kang CJ, Kim WB, Kim D and Oh U (1999) Capsaicin binds to the intracellular domain of the capsaicin-activated ion channel. *J Neurosci* 19:529-538.

Liu L and Simon SA (1997) Capsazepine, a vanilloid receptor antagonist, inhibits nicotinic acetylcholine receptors in rat trigeminal ganglia. *Neurosci Lett* 228:29-32.

Nagy I, Santha P, Jancso G and Urban L (2004) The role of the vanilloid (capsaicin) receptor (TRPV1) in physiology and pathology. *Eur J Pharmacol* 500:351-369.

JPET #84103

Planells-Cases R, Aracil A, Merino JM, Gallar J, Perez-Paya E, Belmonte C, Gonzalez-Ros JM and Ferrer-Montiel AV (2000) Arginine-rich peptides are blockers of VR-1 channels with analgesic activity. *FEBS Lett* 481:131-136.

Premkumar LS and Ahern GP (2000) Induction of vanilloid receptor channel activity by protein kinase C. *Nature* 408:985-990.

Smart D, Jerman JC, Gunthorpe MJ, Brough SJ, Ranson J, Cairns W, Hayes PD, Randall AD and Davis JB (2001) Characterisation using FLIPR of human vanilloid VR1 receptor pharmacology. *Eur J Pharmacol* 417:51-58.

Swanson DM, Dubin AE, Shah C, Nasser N, Chang L, Dax SL, Jetter M, Breitenbucher JG, Liu C, Mazur C, Lord B, Gonzales L, Hoey K, Rizzolio M, Bogenstaetter M, Codd EE, Lee DH, Zhang S-P, Chaplan SR and Carruthers NR (2005) Identification and Biological Evaluation of 4-(3-Trifluoromethylpyridin-2-yl)piperazine-1-carboxylic Acid (5-Trifluoromethylpyridin-2-yl)amide, a high affinity TRPV1 (VR1) vanilloid receptor antagonist. *J Med Chem* 48:1857-1872.

Tominaga M, Caterina MJ, Malmberg AB, Rosen TA, Gilbert H, Skinner K, Raumann BE, Basbaum AI and Julius D (1998) The cloned capsaicin receptor integrates multiple pain-producing stimuli. *Neuron* 21:531-543.

Toth A, Blumberg PM, Chen Z and Kozikowski AP (2004) Design of a high-affinity competitive antagonist of the vanilloid receptor selective for the calcium entry-linked receptor population. *Mol Pharmacol* 65:282-291.

Valenzano KJ, Grant ER, Wu G, Hachicha M, Schmid L, Tafesse L, Sun Q, Rotshteyn Y, Francis J, Limberis J, Malik S, Whittemore ER and Hodges D (2003) N-(4-tertiarybutylphenyl)-4-(3-chloropyridin-2-yl)tetrahydropyrazine - 1(2H)-carbox-amide (BCTC), a novel, orally effective vanilloid receptor 1

JPET #84103

antagonist with analgesic properties: I. in vitro characterization and pharmacokinetic properties. *J Pharmacol Exp Ther* 306:377-386.

Vellani V, Mapplebeck S, Moriondo A, Davis JB and McNaughton PA (2001) Protein kinase C activation potentiates gating of the vanilloid receptor VR1 by capsaicin, protons, heat and anandamide. *J Physiol* 534:813-825.

Vyklicky L, Lyfenko A, Kuffler DP and Vlachova V (2003) Vanilloid receptor TRPV1 is not activated by vanilloids applied intracellularly. *Neuroreport* 14:1061-1065.

Wahl P, Foged C, Tullin S and Thomsen C (2001) Iodo-resiniferatoxin, a new potent vanilloid receptor antagonist. *Mol Pharmacol* 59:9-15.

Wang Y, Szabo T, Welter JD, Toth A, Tran R, Lee J, Kang SU, Suh YG, Blumberg PM and Lee J (2002) High affinity antagonists of the vanilloid receptor. *Mol Pharmacol* 62:947-956. Erratum in *Mol Pharmacol* (2003) 63:958.

Witte DG, Cassar SC, Masters JN, Esbenshade T and Hancock AA (2002) Use of a fluorescent imaging plate reader-based calcium assay to assess pharmacological differences between the human and rat vanilloid receptor. *J Biomol Screen* 7:466-475.

## ***Legends For Figures***

**Fig. 1. Activation of TRPV1-mediated increased intracellular  $\text{Ca}^{2+}$  by different stimuli.** Representative changes in intracellular calcium concentration following activation of the human TRPV1-mediated  $\text{Ca}^{2+}$  flux in HEK293 cells. Solid lines represent hTRPV1-expressing HEK293 cells and dashed lines represent untransfected (Null) cells. An arrow indicates addition time of the agonist. Basal fluorescence ( $\sim 10,000$  RFU) was subtracted from total fluorescence as indicated in Methods, and data are represented in arbitrary relative fluorescence units (RFU). The cells were stimulated by 50 nM capsaicin (**A**), 3  $\mu\text{M}$  NADA (**B**), 10  $\mu\text{M}$  anandamide (**C**) or pH 5.5 (**D**).

**Fig. 2. Concentration-effect curves of activation of TRPV1-mediated increased intracellular  $\text{Ca}^{2+}$  by different stimuli.** (**A**) Representative concentration-effect curves for capsaicin ( $\text{EC}_{50} = 36$  nM) NADA ( $\text{EC}_{50} = 2870$  nM) and anandamide ( $\text{EC}_{50} = 8650$  nM). (**B**) Representative concentration-effect curve for acid activation of the human TRPV1-mediated  $\text{Ca}^{2+}$  flux in HEK293 cells or untransfected HEK293 cells (Null cells).  $\text{EC}_{50}$  value for the acid activation of TRPV1 was approximately pH 5.5. Basal fluorescence ( $\sim 10,000$  RFU) was subtracted from total fluorescence as indicated in Methods, and data are expressed as a % of maximal response.

JPET #84103

**Fig. 3. Chemical structures of TRPV1 antagonists.** (A), A-425619 (1-isoquinolin-5-yl-3-(4-trifluoromethyl-benzyl)-urea); (B), 5-Iodo-resiniferatoxin; (C), capsazepine and (D), ruthenium red.

**Fig. 4. A-425619 potently blocks TRPV1 activation by a variety of stimuli.** Antagonism of the TRPV1-mediated increased intracellular  $\text{Ca}^{2+}$  was performed by adding the antagonists before agonist stimulation, as described in Methods. Data are represented in % of maximal response (control) minus basal fluorescence. All antagonists were assayed in parallel under the same conditions against 50 nM capsaicin (A), 3  $\mu\text{M}$  NADA (B), 10  $\mu\text{M}$  anandamide (C) or acid (pH 5.5)(D). See Table 1 for a summary of the  $\text{pIC}_{50}$  values.

**Fig. 5. Concentration-dependent inhibition of native TRPV1 channels by A-425619.** (A) Representative current traces illustrating the concentration-dependent inhibition of 1  $\mu\text{M}$  capsaicin-activated inward currents by 3, 10 and 100 nM A-425619 in a single cultured rat DRG neuron. Capsaicin current amplitudes returned to > 80% of control following 4-6 minutes of washout of the antagonist (gray line). (B) Average normalized data plotted as a function of A-425619 concentration and fitted with a logistic equation ( $\text{IC}_{50} = 8.6 \text{ nM}$ , and Hill slope of  $-0.8$ ). Data are the mean  $\pm$  S.E.M.

**Fig. 6. A-425619 is a competitive antagonist at TRPV1.** (A) Concentration-effect curves for capsaicin-induced increased intracellular  $\text{Ca}^{2+}$  in

JPET #84103

the presence of increasing concentrations of A-425619. Curves are plotted as a % of the maximal response obtained in the absence of antagonist. **(B)** Schild plot analysis of the antagonism produced by A-425619. **(C and D)**, concentration-response curves for capsaicin activation of TRPV1 in the presence of increasing concentrations of capsazepine and ruthenium red, respectively. Curves are plotted as a % of the maximal control response obtained in the absence of the antagonist.

**Fig. 7. A-425619 is a potent antagonist at sensitized TRPV1.**

Concentration-effect curves for capsaicin-induced increased intracellular  $\text{Ca}^{2+}$  in the presence of increasing concentrations of A-425619 were performed in the presence of 100 nM PDBu **(A)** or pH 6.0 **(B)**, as described in Methods. Curves are plotted as a % of the maximal response obtained in the absence of antagonist. **(C)** Schild plot analysis of the antagonism produced by A-425619 yielded  $\text{pA}_2$  values of  $0.8 \pm 0.3$  nM (PDBu-sensitized) and  $4.3 \pm 1.9$  nM (Acid-sensitized).  $\text{pA}_2$  of A-425619 for naive TRPV1 (filled circles) corresponds to that shown in Fig. 6 ( $2.5 \pm 0.6$  nM).

**Fig. 8. Concentration-dependent antagonism of PDBu-sensitized**

**TRPV1.** Antagonists were added to PDBu-sensitized cells before the challenge with 8.5 nM capsaicin ( $\sim \text{EC}_{50}$ ), as described in Methods. Data are represented in % of maximal response (control) minus basal fluorescence.  $\text{pIC}_{50}$  values for tested antagonists are summarized in Table 3.

JPET #84103

**Fig. 9. Effect of A-425619 on the heat-evoked increased intracellular calcium.** (A) Representative tracings of the activation by heat (38°C) of the human TRPV1-mediated  $\text{Ca}^{2+}$  flux in HEK293 cells. Solid lines represent TRPV1-expressing HEK293 cells and dashed lines represent untransfected (Null) cells. Cells were untreated (gray lines) or treated (black lines) with 100 nM PDBu for 20 min before addition of the stimulus (indicated by an arrow). (B) Dose-dependent antagonism of heat (38°C)-evoked TRPV1-mediated  $\text{Ca}^{2+}$  flux after pretreatment with 100 nM PDBu for 20 min.  $\text{pIC}_{50}$  values of the antagonists are summarized in Table 3.

JPET #84103

**Table 1. Functional potencies of antagonists at hTRPV1**

	pIC <sub>50</sub> (M) (Hill Slope)			
	50 nM Capsaicin	3 μM NADA	10 μM Anandamide	Acid (pH 5.5)
<b>A-425619</b>	8.32 ± 0.04 (1.59 ± 0.19)	8.42 ± 0.04 (1.50 ± 0.10)	8.52 ± 0.07 (1.61 ± 0.20)	8.72 ± 0.09 (2.01 ± 0.26)
<b>Capsazepine</b>	6.85 ± 0.04 (1.95 ± 0.18)	6.89 ± 0.06 (2.01 ± 0.19)	6.84 ± 0.06 (2.61 ± 0.41)	7.38 ± 0.13 (1.20 ± 0.17)
<b>Ruthenium red</b>	6.30 ± 0.02 (1.72 ± 0.19)	6.43 ± 0.04 (2.19 ± 0.27)	6.49 ± 0.13 (1.35 ± 0.30)	6.41 ± 0.02 (3.70 ± 0.73)
<b>I-RTX</b>	7.34 ± 0.13 (2.02 ± 0.43)	7.59 ± 0.11 (1.71 ± 0.39)	7.20 ± 0.11 (2.19 ± 0.50)	7.14 ± 0.14 (2.20 ± 0.66)

Potencies are shown as mean pIC<sub>50</sub> values ± S.E.M. for 5-16 determinations

Hill Slope ± S.E.M. are presented in parentheses

JPET #84103

**Table 2. Pharmacological selectivity of A-425619**

Target	ligand	~IC <sub>50</sub> (μM)	Target	ligand	~IC <sub>50</sub> (μM)
Adenosine A <sub>1</sub>	[ <sup>3</sup> H]DPCPX	> 10	Angiotensin AT <sub>1</sub>	[ <sup>125</sup> I][Sar <sup>1</sup> ,Ile <sup>8</sup> ]-ATII	> 10
Adenosine A <sub>2A</sub>	[ <sup>3</sup> H]CGS 21680	> 10	Angiotensin AT <sub>2</sub>	[ <sup>125</sup> I]CGP 42112A	> 10
Adenosine A <sub>3</sub>	[ <sup>125</sup> I]AB-MECA	> 10	Bombesin	[ <sup>125</sup> I][Tyr <sup>4</sup> ]bombesin	> 10
Adrenergic α <sub>1</sub>	[ <sup>3</sup> H]Prazosin	> 10	Bradykinin B2	[ <sup>3</sup> H]NPC 17731	> 10
Adrenergic α <sub>2</sub>	[ <sup>3</sup> H]RX821002	> 10	CCKA	[ <sup>3</sup> H]Devazepide	> 10
Adrenergic β <sub>1</sub>	[ <sup>3</sup> H](-)-CGP 12177	> 10	CCKB	[ <sup>3</sup> H]CCK-8	> 10
Adrenergic β <sub>2</sub>	[ <sup>3</sup> H](-)-CGP 12177	> 10	Endothelin ET <sub>A</sub>	[ <sup>125</sup> I]Endothelin-1	> 10
ANP	[ <sup>125</sup> I]ANP	> 10	Endothelin ET <sub>B</sub>	[ <sup>125</sup> I]Endothelin-1	> 10
Cannabinoid CB <sub>1</sub>	[ <sup>3</sup> H]Win 55212-2	> 10	Galanin GAL1	[ <sup>125</sup> I]Galanin	> 10
Cannabinoid CB <sub>2</sub>	[ <sup>3</sup> H]Win 55212-2	> 10	PDGF	[ <sup>125</sup> I]PDGF BB	> 10
Dopamine D1	[ <sup>3</sup> H]SCH 23390	> 10	Melatonin ML1	[ <sup>125</sup> I]iodomelatonin	> 10
Dopamine D2	[ <sup>3</sup> H]Spiperone	> 10	Neurokinin NK <sub>1</sub>	[ <sup>125</sup> I][Sar <sup>9</sup> ,Met(O <sub>2</sub> ) <sup>11</sup> ]-S	> 10
Dopamine D3	[ <sup>3</sup> H]Spiperone	> 10	Neurokinin NK <sub>2</sub>	[ <sup>125</sup> I]NKA	> 10
Dopamine D4.4	[ <sup>3</sup> H]Spiperone	> 10	Neurokinin NK <sub>3</sub>	[ <sup>125</sup> I][MePhe <sup>7</sup> ]-NKB	> 10
Dopamine D5	[ <sup>3</sup> H]SCH 23390	> 10	Neuropeptide Y1	[ <sup>125</sup> I]peptide YY	> 10
GABA	[ <sup>3</sup> H]GABA	> 10	Neuropeptide Y2	[ <sup>125</sup> I]peptide YY	> 10
IL-8B (CXCR2)	[ <sup>125</sup> I]IL-8	> 10	Neurotensin NT1	[ <sup>125</sup> I]Neurotensin	> 10
TNFα	[ <sup>125</sup> I]TNFα	> 10	Somatostatin	[ <sup>125</sup> I]Tyr <sup>11</sup> -somatostatin	> 10
CCR1	[ <sup>125</sup> I]MIP-1α	> 10	VIP <sub>1</sub> (VPAC <sub>1</sub> )	[ <sup>125</sup> I]VIP	> 10
Histamine H1	[ <sup>3</sup> H]Pyrilamine	> 10	Vasopressin V1a	[ <sup>3</sup> H]AVP	> 10
Histamine H2	[ <sup>125</sup> I]APT	> 10	NE transporter	[ <sup>3</sup> H]Nisoxetine	> 10
Muscarinic M1	[ <sup>3</sup> H]Pirenzepine	> 10	DA uptake	[ <sup>3</sup> H]GBR 12935	> 10
Muscarinic M2	[ <sup>3</sup> H]AF-DX384	> 10	BenzodiazepineCentral	[ <sup>3</sup> H]Flunitrazepam	> 10
Muscarinic M3	[ <sup>3</sup> H]4-DAMP	> 10	BenzodiazepinePeripheral	[ <sup>3</sup> H]PK 11195	5
Muscarinic M4	[ <sup>3</sup> H]4-DAMP	> 10	AMPA	[ <sup>3</sup> H]AMPA	> 10
Muscarinic M5	[ <sup>3</sup> H]4-DAMP	> 10	Kainate	[ <sup>3</sup> H]Kainic acid	> 10
Opioid δ2	[ <sup>3</sup> H]DADLE	> 10	NMDA	[ <sup>3</sup> H]CGP 39653	> 10
Opioid κ	[ <sup>3</sup> H]U 69593	> 10	Ca <sup>2+</sup> channel DHP site	[ <sup>3</sup> H]PN200-110	> 10
Opioid μ	[ <sup>3</sup> H]DAMGO	> 10	Ca <sup>2+</sup> channel diltiazem site	[ <sup>3</sup> H]Diltiazem	> 10
ORL1	[ <sup>3</sup> H]Nociceptin	> 10	Ca <sup>2+</sup> channel verapamil site	[ <sup>3</sup> H]D 888	> 10
PACAP PAC <sub>1</sub>	[ <sup>3</sup> H]PACAP <sub>1-27</sub>	> 10	Ca <sup>2+</sup> channel N	[ <sup>125</sup> I]ω-conotoxin	> 10
P2X	[ <sup>3</sup> H]α,βMeATP	> 10	K <sup>+</sup> channel (volt. dependent)	[ <sup>125</sup> I]Dendrotoxin	> 10
P2Y	[ <sup>35</sup> S]dATPαS	> 10	K <sup>+</sup> channel (Ca <sup>2+</sup> dependent)	[ <sup>125</sup> I]Apmin	> 10
Serotonin 5-HT <sub>1A</sub>	[ <sup>3</sup> H]8-OH-DPAT	> 10	Na <sup>+</sup> channel (Site 2)	[ <sup>3</sup> H]Batrachotoxinin	> 10
Serotonin 5-HT <sub>1B</sub>	[ <sup>3</sup> H]CYP	> 10	Cl <sup>-</sup> ionophore	[ <sup>35</sup> S]TBPS	> 10
Serotonin 5-HT <sub>2A</sub>	[ <sup>3</sup> H]Ketanserin	> 10	Glycine (strychnine-sensitive)	[ <sup>3</sup> H]Strychnine	> 10
Serotonin 5-HT <sub>2C</sub>	[ <sup>3</sup> H]Mesulergine	> 10	Glycine (strychnine-insensitive)	[ <sup>3</sup> H]MDL 105,519	> 10
Serotonin 5-HT <sub>3</sub>	[ <sup>3</sup> H]BRL 43694	> 10	MAO-A	[ <sup>3</sup> H]Ro41-1049	> 10
Serotonin 5-HT <sub>5A</sub>	[ <sup>3</sup> H]LSD	> 10	MAO-B	[ <sup>3</sup> H]Ro-19-6327	> 10
Serotonin 5-HT <sub>6</sub>	[ <sup>3</sup> H]LSD	> 10	Sigma	[ <sup>3</sup> H]DTG	10
Serotonin 5-HT <sub>7</sub>	[ <sup>3</sup> H]LSD	> 10	Sigma <sub>2</sub>	[ <sup>3</sup> H]DTG	> 10
Sigma <sub>1</sub>	[ <sup>3</sup> H]Pentazocine	> 10			

JPET #84103

**Table 3. Functional potencies of antagonists at sensitized hTRPV1**

	pIC <sub>50</sub> (M) (Hill Slope)			
	PDBu- sensitized			
	8.5 nM Capsaicin	Heat (38°C)		
<b>A-425619</b>	8.05 ± 0.06 (2.10 ± 0.27)	8.70 ± 0.06	(1.24 ± 0.34)	
<b>Capsazepine</b>	6.83 ± 0.13 (1.74 ± 0.30)	7.00 ± 0.06	(1.90 ± 0.40)	
<b>Ruthenium red</b>	6.48 ± 0.05 (1.63 ± 0.25)	6.30 ± 0.06	(2.70 ± 1.66)	
<b>I-RTX</b>	6.84 ± 0.09 (3.20 ± 0.52)	7.27 ± 0.05	(2.83 ± 0.83)	

Potencies are shown as mean pIC<sub>50</sub> values ± S.E.M. for 5-16 determinations

Hill Slope ± S.E.M. are presented in parentheses

Figure 1

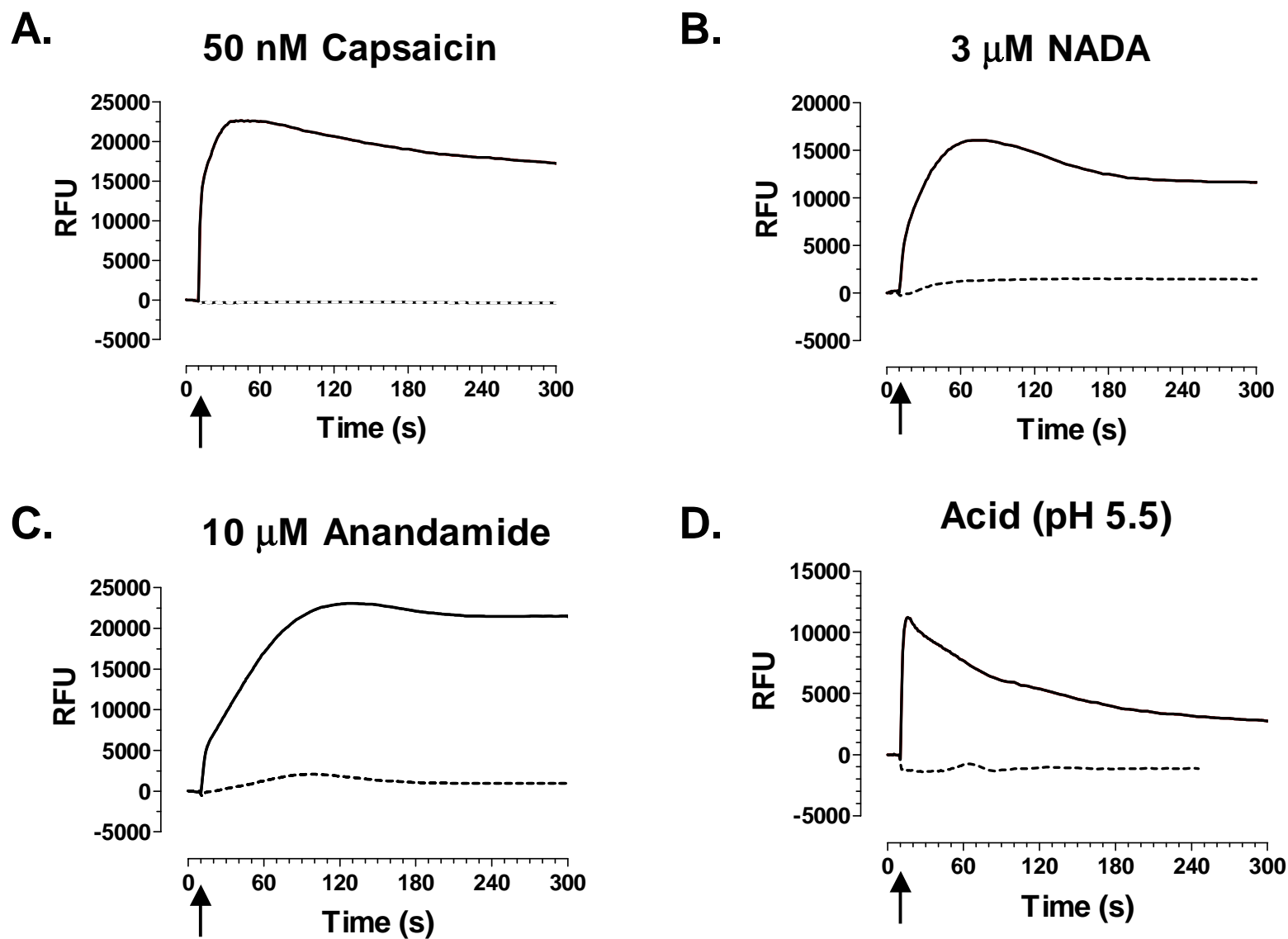
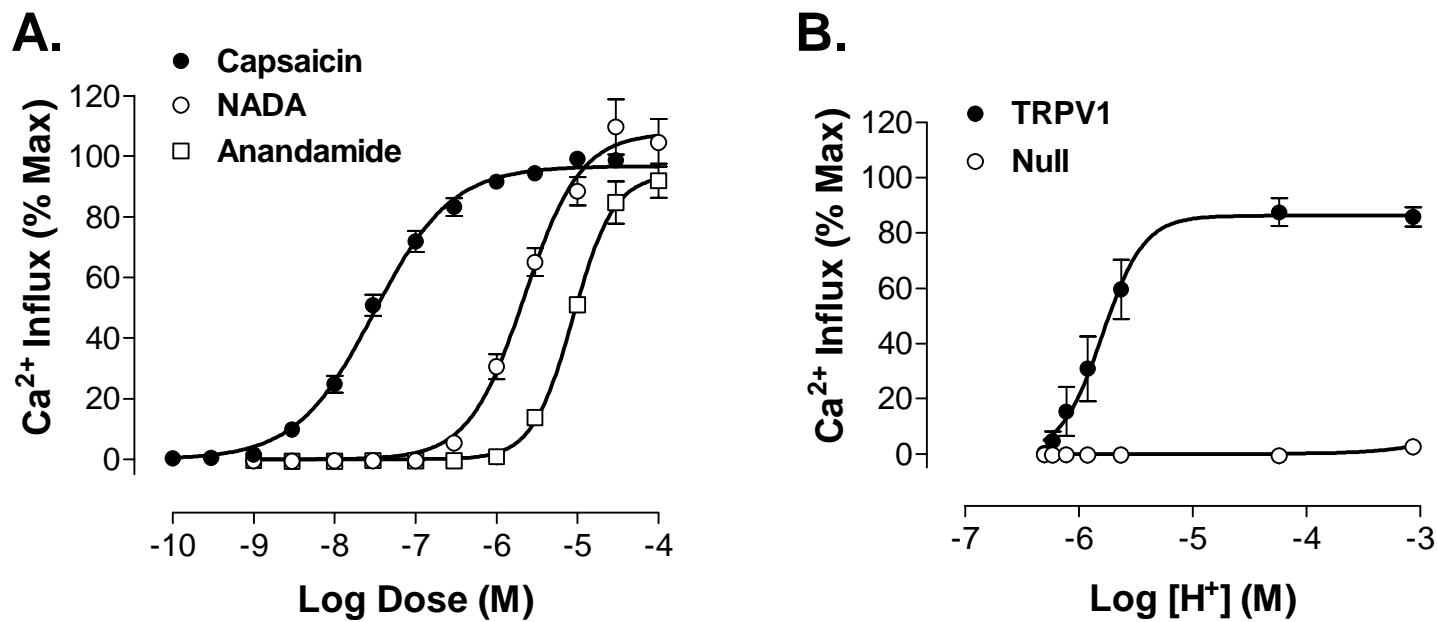
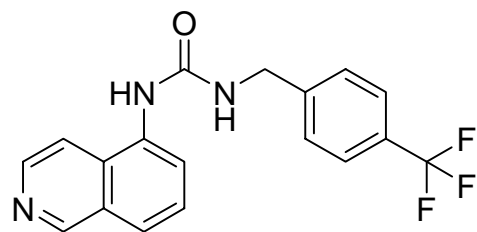


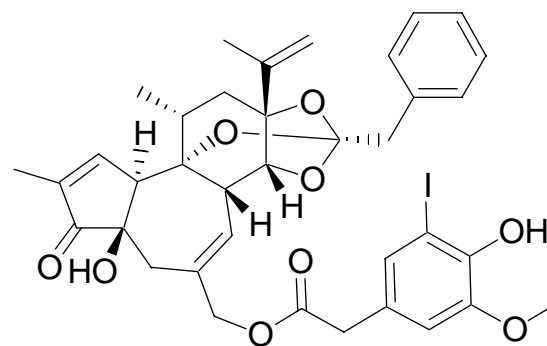
Figure 2



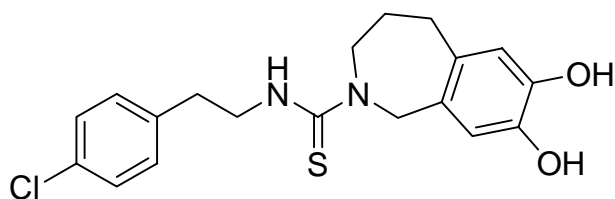
**Figure 3**



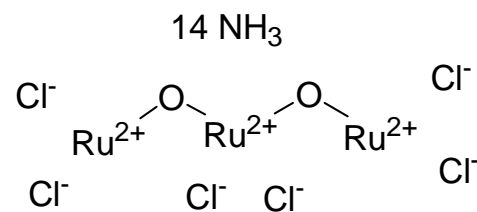
**(A) A-425619**



**(B) 5-Iodo-Resiniferatoxin**



**(C) Capsazepine**



**(D) Ruthenium Red**

**Figure 4**

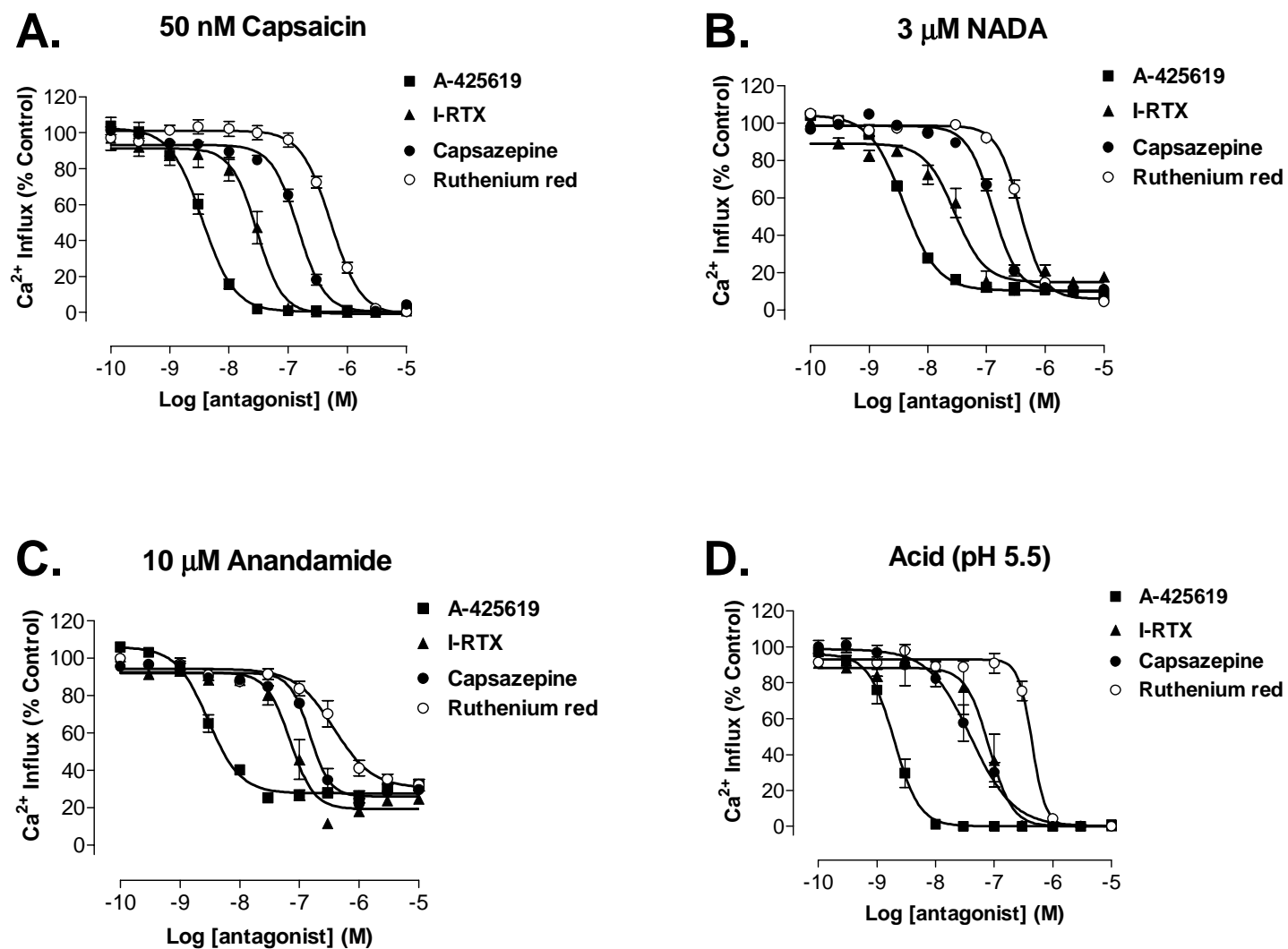


**Figure 5**

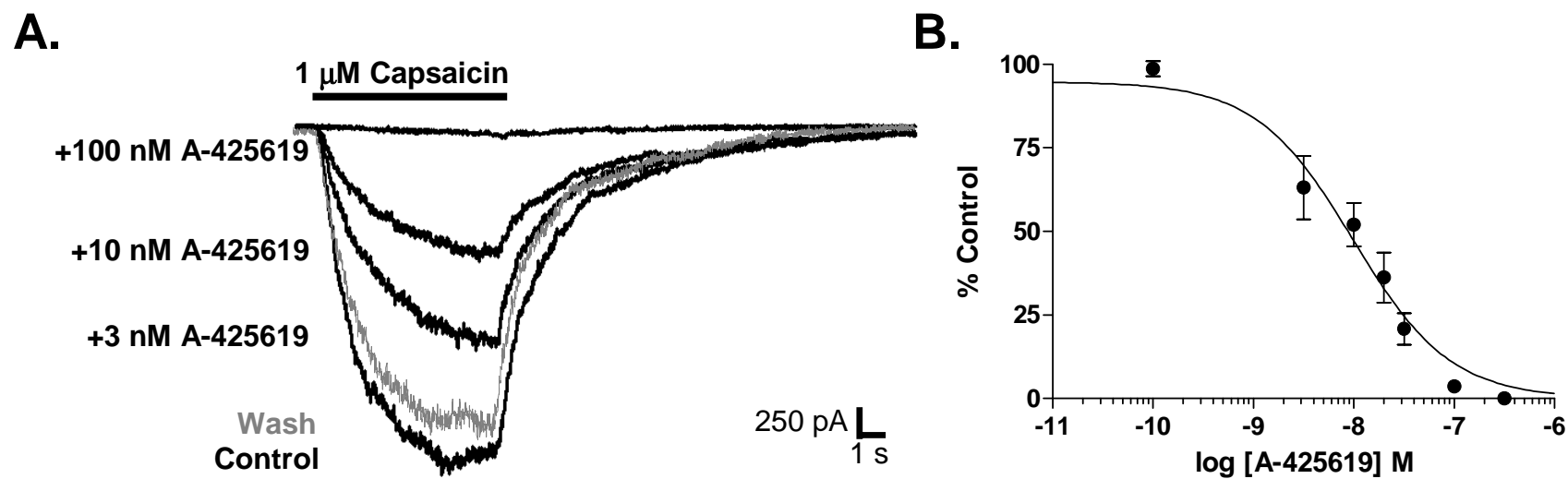


**Figure 6**

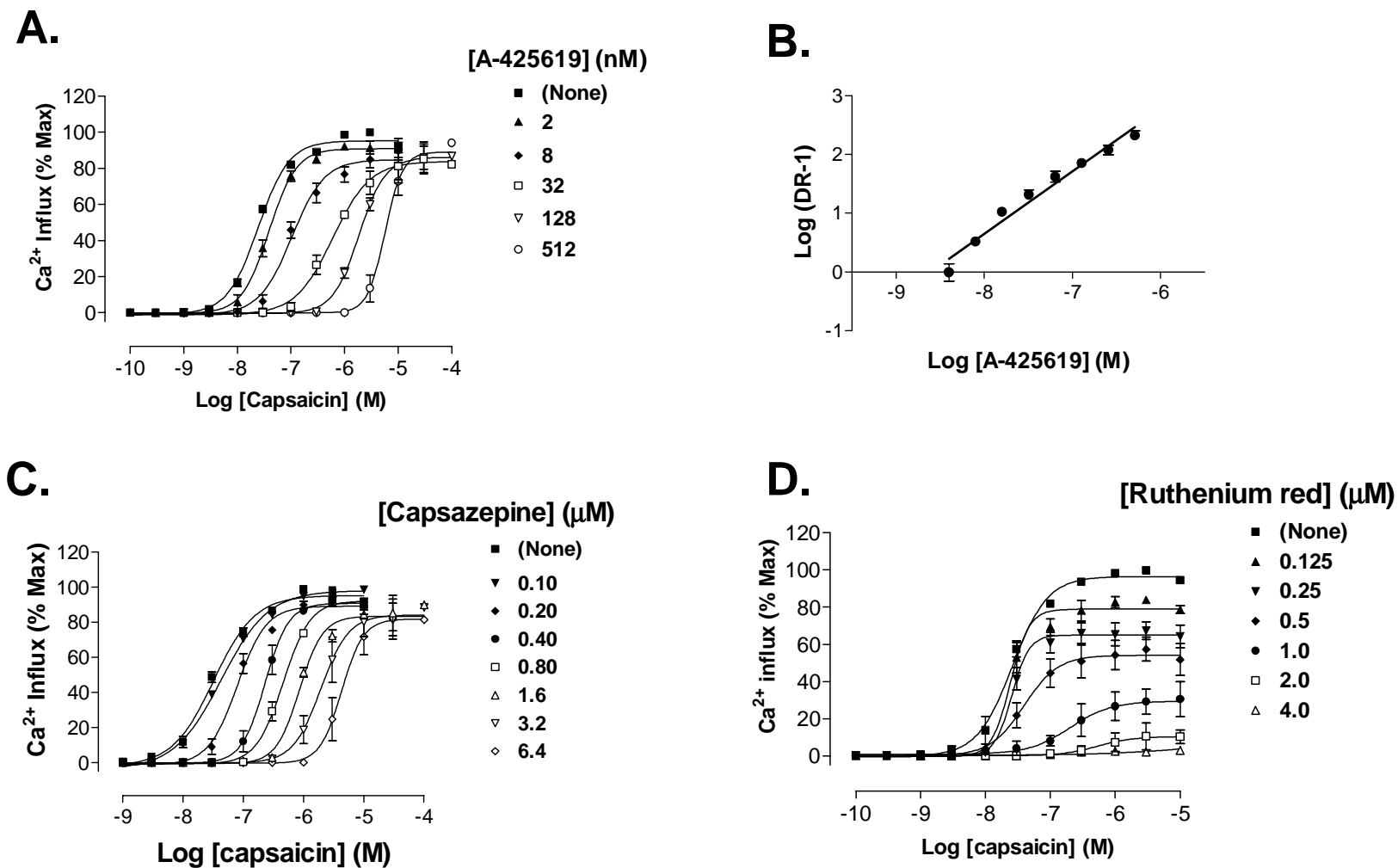


**Figure 7**

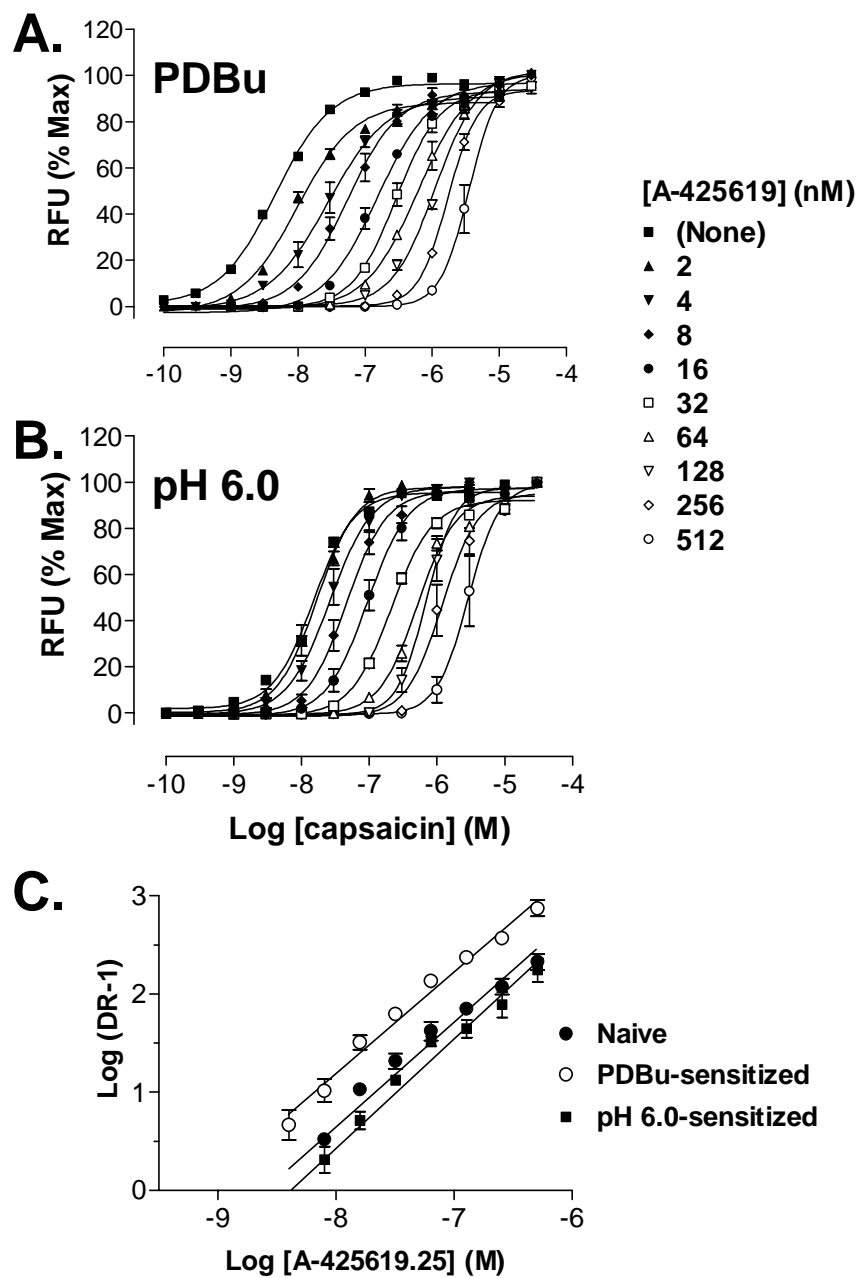
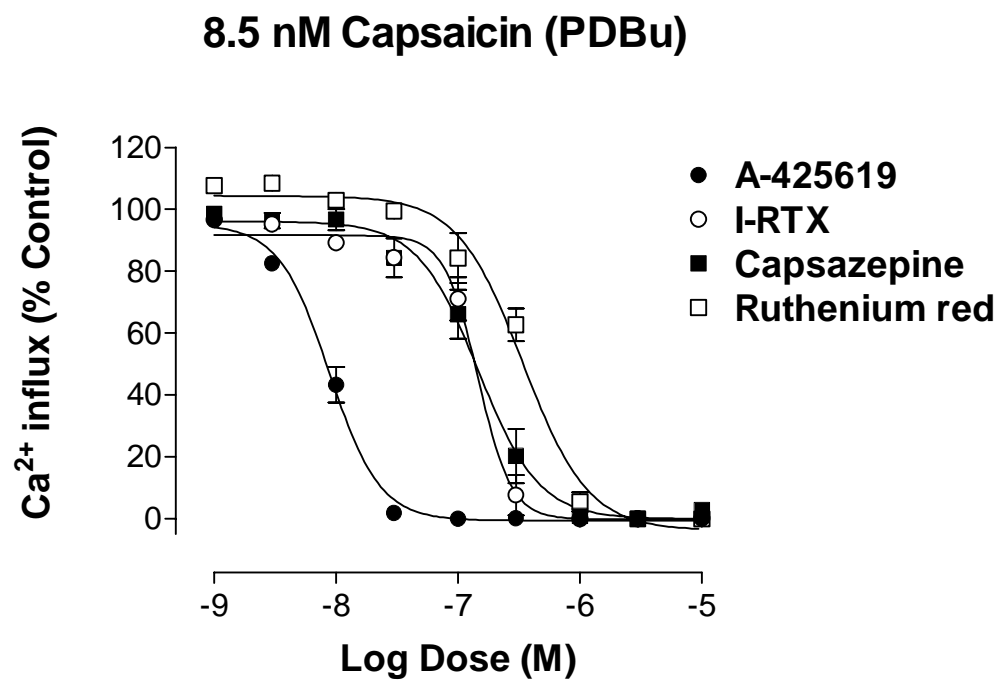


Figure 8



**Figure 9**

